Kinetics of Enthalpy Relaxation upon Physical Aging in Glassy Main-Chain Nematic Polymers

C. B. McGowan

Department of Chemistry, Wellesley College, Wellesley, Massachusetts 02181

D. Y. Kim† and R. B. Blumstein*

Polymer Science Program, Department of Chemistry, University of Massachusetts, Lowell, Lowell, Massachusetts 01854

Received December 17, 1991; Revised Manuscript Received May 11, 1992

ABSTRACT: Kinetics of enthalpy relaxation upon physical aging of thermotropic nematic main-chain polyesters below their glass transition temperature is followed by DSC. Aging temperatures T_a are typically in the range $T_g - T_a = 10$–20 K. Two fully aromatic semiflexible polymers and two inherently flexible polymers based on mesogens connected via aliphatic spacers are studied. In the latter case, the chains are randomly coiled in the isotropic melt but behave as semiflexible, rodlike materials in the nematic phase. A fractionated polystyrene is used as a reference conventional glass. Characteristic relaxation times are longer in LCP glasses than in PS and are strongly dependent on molecular mass and distribution. Relaxation times display an Arrhenius dependence within our range of aging temperatures, with a high value of apparent activation energy. Relaxation seems to be strongly nonlinear, e.g., strongly dependent on the instantaneous structure of the glass. The parameter characterizing distribution of relaxation times is measured for various temperatures and chain lengths. Molecular mass effects appear to be dominant, rather than inherent chain flexibility, but our experimental base at present does not justify a truly quantitative discussion of data.

Introduction

The backbone moieties in thermotropic main-chain liquid crystalline polymers (LCPs) may either be fully aromatic or comprise flexible spacer groups in a rigid–flexible (RF) sequencing. Although polymers with both types of molecular architecture have been abundantly studied in recent years, investigation of their behavior in the mesophase glass is lagging, with only a few studies of LCP glass transition by calorimetry[1-6] or dynamic methods.[7]

This paper presents an attempt at a systematic correlation between macroscopic properties of LCP glasses, on the one hand, and their molecular order and supramolecular architecture, on the other; it belongs to a series describing a calorimetric investigation of the glass transition in thermotropic nematic main-chain polyesters.[3,4] Kinetics of enthalpy relaxation upon physical aging of several nematic polymer glasses is investigated by differential scanning calorimetry (DSC). Two sets of samples are studied: inherently flexible polyalkanoates with RF sequencing and inherently semiflexible fully aromatic chains. The former are poly[oxy(3-methyl-1,4-phenylene)-azoxy-(2-methyl-1,4-phenylene)oxy(α,ω-dioxo-α,ω-alkanediyls)] with spacer length $(CH_2)_7$ and $(CH_2)_{10}$ which are designated as polymers AZA9 and DDA9, respectively. The latter are poly[oxy(chloro-1,4-phenylene)oxycarbonyl-[(trifluoromethyl)-1,4-phenylene]carbonyl] (PTFC) and Du Pont polyester HX2000. We begin by recalling briefly previous results concerning molecular order in polymers AZA9, DDA9, and PTFC (the structure of polymer HX2000 is still proprietary). That is followed by a description of our computational methods and a summary of experimental results.

Polymers AZA9 and DDA9 belong to a homologous series which has been extensively studied in our laboratory, for spacer lengths ranging from 4 to 20 methylene units. Phase behavior, molecular order, and viscoelastic properties have been investigated in detail (see ref 8 and references therein for a review). The chains are inherently flexible; e.g., they behave as random coils in the isotropic melt or solution. Strong pretransitional effects are observed upon cooling from the isotropic (I) state, and the isotropic–nematic (I/N) transition is characterized by a drastic orientational and conformational ordering of chains. Mesogen and spacer order are strongly coupled. Spacer extension and concomitant chain rigidity increase as the temperature is lowered and/or as the molecular mass is increased. The series is characterized by a strong, sustained odd–even oscillation of nematic order (higher for n = even than for n = odd) that affects virtually every physical property. One notable exception is found in the inverse, even–odd oscillation in the glass transition temperature, for which we currently have no explanation.

As T_g is approached upon cooling across the nematic phase, the mesogen order parameter reaches a value of 0.8–0.9 and the spacer order approaches that observed in the crystal. The resulting highly ordered nematic glasses (below T_g) and "rubbery" phases of extended chains (above T_g) have interesting material properties: high values of the tensile modulus, which decrease by only 30–50% as T_g is crossed on heating,[9,10] in contrast to the usual drop of several decades that is observed in conventional glasses. Macroscopic alignment is easily achieved by application of external fields, and cross-linking following sample alignment provides systems with biaxial strength.[10]

In a previous DSC study of AZA9 and DDA9, influence of spacer parity and molecular mass on the glass transition temperature, the shape of the heat capacity curve Cp(T) and the heat capacity increment at T_g [ΔCp = Cp(liquid) – Cp(solid)] were investigated for fractionated samples.[3] The value of ΔCp decreases steadily with increasing $\bar{M}_n$, within the range of chain lengths studied to date (from "siamese twin" dimers to $\bar{M}_n$ = 20 000). The amplitude of this effect is in-phase with the observed odd–even oscillation in the level of nematic order, with a drop in ΔCp of ca. 30% and 50% respectively for AZA9 and DDA9. Heat capacity of the solid below T_g is independent of molecular mass, but the liquid Cp decreases steadily. In

* To whom correspondence should be addressed.
† Present address: KIST. Polymer Materials Lab, Soeul, Korea.

0024-9297/92/2225-4658$03.00/0

contrast to this decrease, one may note that Cp(liquid) of *n*-paraffins at 25 °C (*n*-nonane through *n*-hexadecane) is constant[11] and exactly the same as for polyethylene.[12]

The observed decrease in ΔCp is quite unexpected, as the dynamics of devitrification involve a very local motion. As chain length increases, the liquid mesophase structure appears to progressively change to a "strong" liquid which exhibits a small value of ΔCp due to "restrictions on the configurational states which the system can adopt".[13] In our case, the data may be interpreted as reflecting a continuous increase in the level of molecular ordering and chain rigidity over a range of molecular masses extending well beyond the commonly recognized "plateau" value at $\overline{DP} \approx 10$. Such an increase is suggested by our experimental data from broadly based studies, including X-ray,[8] NMR, magnetic susceptibility,[14] and small-angle neutron scattering.[15] We interpret the observed decrease in ΔCp, which reflects a decrease in Cp(liquid) alone, as a natural consequence of the rigidification of the liquid mesophase brought about by a decrease of orientational fluctuations coupled with increased conformational order of chains.

While DDA9 and AZA9 are inherently flexible, albeit behaving as semiflexible chains in the nematic field, PTFC is inherently semiflexible. It belongs to a family of para-linked polyesters based on trifluoromethyl substitution in a phenyl and/or biphenyl moiety.[16] These structural features preserve molecular rigidity: the Mark–Houwink coefficient in the intrinsic viscosity–molecular mass relation is in the range 1.0–1.1; the nematic order parameter in the liquid mesophase behaves athermally, with a value $S \approx 0.85$,[17] about the same as in the nematic glass of a related polymer.[16] PTFC and related LCPs are interesting materials for the study of mesophase glasses, because they do not crystallize, remaining fully amorphous both above and below T_g. Although the structure of Du Pont copolyester HX2000 is not yet published, it too is a fully aromatic thermotropic structure where crystallization may be easily avoided.[18]

When liquids are cooled below their glass transition under normal experimental conditions, the resulting glass is not in a state of equilibrium and will undergo structural relaxation upon isothermal aging below T_g. This process is reflected in a time dependence of properties such as enthalpy, specific volume, or refractive index. Kinetics of structural relaxation is nonexponential and nonlinear: it is characterized by a spectrum of relaxation times, which depend on the departure from equilibrium (e.g., the instantaneous "structure" of the glass) as well as aging temperature. Interpretation of experimental results is often based on a phenomenological model developed independently by Moynihan,[19] Kovacs,[20] and their coworkers, on the foundation of analysis by Tool[21] and Narayanaswami.[22] The spectrum of relaxation times may be conveniently represented by the Kohlrausch–Williams–Watts (KWW) relaxation function

$$\phi(t_a) = e^{-(t_a/\tau)^\beta} \tag{1}$$

where t_a is the aging time, β ($0 < \beta \leq 1$) is a parameter that specifies the shape of the spectrum, and τ a reference relaxation time.

The nonlinearity of the relaxation response reflects the time dependence of τ caused by a continuously changing structure of the glass. Tool[21] expressed this variation of τ by introducing the concept of fictive temperature T_f such that $\tau = \tau(T_a, T_f)$, where T_a is the aging temperature and approach toward equilibrium is monitored in terms of the isothermal time dependence of T_f.

A frequently used form of τ is the empirical Narayanaswami equation

$$\tau = A \exp\left[\frac{x\Delta h^*}{RT_a} - \frac{(1-x)\Delta h^*}{RT_f}\right] \tag{2}$$

which partitions τ between T_a and T_f via the parameter x ($0 < x \leq 1$). In eq 2, A is a constant and Δh^* represents the activation energy in the equilibrium state above T_g.

Four adjustable parameters (A, Δh^*, x, and β) are required in order to account for structural relaxation in the framework of the above model. The reader is referred to refs 23–27 and citations therein for a more thorough introduction and discussion of computational methods, since in the present study we use a simplex parametrization based on eqs 1 and 2 (see below). Enthalpy relaxation upon sub-T_g aging of several LCPs is followed by DSC. The relaxation function is expressed as

$$\phi(t_a) = \frac{\Delta H(T_a,t_\infty) - \Delta H(T_a,t_a)}{\Delta H(T_a,t_\infty)} \tag{3}$$

where $\Delta H(T_a,t_a)$ and $\Delta H(T_a,t_\infty)$ represent the enthalpy lost upon aging for a time t_a and upon reaching the equilibrium structure, respectively. The value of $\Delta H(T_a,t_\infty)$ is measured independently from the heat capacity scan of the unaged sample. The parameters β and τ are extracted from eq 1 by fitting the data to a portion of the relaxation curve over which τ may be considered as independent of time (e.g., the KWW function displays a linear form, as opposed to the generalized form embodied in eq 1). The values of Δh^* and x in eq 2 are extracted in a subsequent step as described below.

In an effort at elucidating influence of chain length and inherent chain flexibility, kinetics of enthalpy relaxation upon physical aging in the glassy state is investigated for several molecular masses of AZA9 and DDA9 and for a single mass of PTFC and HX2000 glasses. A polystyrene standard (PS) is used as a reference material. In addition to our own preliminary study on DDA9 and AZA9,[4] there are only two calorimetric investigations of kinetics of enthalpy recovery in main-chain LCPs, to our knowledge.[5,6] Results presented in refs 5 and 6 will be briefly discussed.

Materials and Methods

Sample preparation and characterization of DDA9 and AZA9 have been described previously (see references cited in ref 8). Synthesis of PTFC has been reported in ref 16, and the structure of copolyester HX2000 is proprietary. Sample molecular masses are listed in Table I, as $\bar{M}_n$ values obtained by GPC. All three DDA9 samples and AZA9M4200 are fractions characterized by a polydispersity index $\bar{M}_w/\bar{M}_n < 1.1$. The DDA9 fractions used here are the same as those in ref 28, where representative GPC chromatograms and the calibration method are illustrated. PTFC, HX2000, and AZA9 samples of mass 8200 and 16 900 are unfractionated, with polydispersity 1.6–2.0. The polystyrene sample is a nearly monodisperse standard.

Heat capacity measurements were carried out on a Perkin-Elmer DSC2C with a TADS data station. Sample weights were in the range 7–12 mg. The absolute heat capacity (Cp) was determined with the Specific Heat Measurement Kit supplied by Perkin-Elmer. The output signal and analysis procedure were calibrated with indium and aluminum oxide (synthetic sapphire). The measured absolute Cp values of aluminum oxide agreed with the National Bureau of Standards values to better than 1%.

Following the approach described in ref 29, the glass transition region is characterized by five temperatures, as illustrated in Figure 1. The width of the major portion of the transition is given by the interval between T_1 and T_2, with T_g corresponding to the half-devitrification point where the experimental heat capacity curve Cp(T) intersects with the midline of the extrapolated solid and liquid lines (Cp(solid) and Cp(liquid)). The

Table I

sample[a]	T_b (K)	T_1 (K)	T_g (K)	T_2 (K)	T_e (K)	$T_e - T_b$	ΔCp (cal/g·K)
AZA9*M*4200	268	284	286.8	292	298	30	0.092
AZA9*M*8200	281	289	292	295.5	305	24	0.093
AZA9*M*16900	283	289	293.5	297.5	305	22	0.081
DDA9*M*2550	264	274.6	278.8	284	294	30	0.114
DDA9*M*6900	266.8	276.7	282	288	296	29	0.066
DDA9*M*11300	267.5	281	285.5	289.5	292	24.5	0.063
PTFC*M*6900	295	341.5	346	351.5	370	75	0.052
HX2000	441	448	463	478	522	81	0.044
PS*M*173000	370	375	378	379	392	22	0.071

[a] The sample designation is followed by the value of molecular mass M ($\bar{M}_n$ value is from GPC). $\bar{M}_n$ for HX2000 is estimated at roughly 10 000.[18]

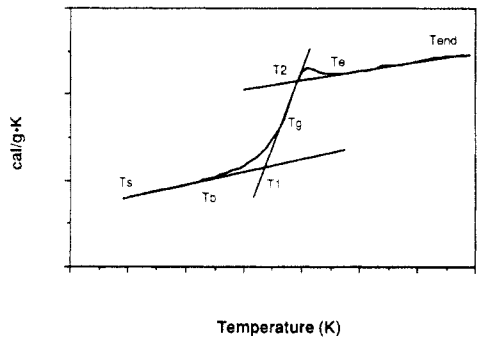

Figure 1. Glass transition region. See text for definitions.

heat capacity increment Cp(liquid) − Cp(solid) at T_g is represented by ΔCp. The total width of the transition is given by $T_e - T_b$, where T_b is the first point of deviation from Cp(solid) and T_e represents the end of the transition, as judged by the return of the curve to the liquid line Cp(liquid). Heat capacities were measured between temperatures T_s and T_{end}, chosen so as to provide an accurate representation of Cp(solid,T) and Cp(liquid,T). The temperature dependence of Cp(solid) and Cp(liquid) is obtained by fitting the solid and liquid portions of Cp(T) or $H(T)$ to a straight line or a second-order polynomial, respectively.

All samples were quenched to the scan starting temperature (T_s) after annealing for 15 min, as follows: DDA9 and AZA9 were held in the isotropic melt at 450 K, some 30–50 °C above their nematic/isotropic transition; PTFC and HX2000 were annealed in the nematic liquid at T_g + 100 and 80 °C, respectively, as their isotropic phase is not accessible without decomposition; the PS standard was similarly held in the liquid phase at T_g + 100 °C. The samples were quenched to T_s at 320 K/min (nominal rate), with the exception of DDA9 fractions which were quenched into liquid nitrogen and then placed in the calorimeter previously equilibrated at T_s = 210 K (crystallization of DDA9 cannot be totally avoided by cooling at 320 K/min[3]).

Aging experiments followed the sequence (1) Cp scan of the unaged sample between T_s and T_{end} (20 K/min), (2) quenching from T_{end} at 320 K/min to the aging temperature (T_a) and aging for a time t_a (minutes), (3) quenching to T_s at 320 K/min and recording Cp of the aged sample (Cp(a)) between T_s and T_{end} (20 K/min), and (4) quenching to T_s at 320 K/min and repeating a base-line, unaged scan. This step was repeated after each aging scan to ensure reproducibility of the unaged Cp curve (Cp(u)).

Aging times (t_a) and/or temperatures (T_a) were varied without removing the sample, in order to minimize errors that might be introduced by repositioning the sample pan. All Cp(u) curves were reproducible, within experimental error on the absolute value of Cp. Reproducibility of data was further checked by repeating several randomly chosen experiments using different samples.

The enthalpy $\Delta H(T_a,t_a)$ lost by aging at temperature T_a for a time t_a is $\Delta H(T_a,t_a) = \int_{T_C}^{T_B}(\mathrm{Cp(a)} - \mathrm{Cp(u)})\,dT$, where the numerical integration limits T_B and T_C are chosen outside the glass transition region as defined by $T_e - T_b$. The values reported for $\Delta H(T_a,t_a)$ are an average over several integration limits (the procedure is similar to that described by Cowie and Ferguson in a study of physical aging of poly(vinyl methyl ether).[30]

Enthalpy lost upon reaching the equilibrium liquid state is obtained from the reference heat capacity scan of the unaged sample by extrapolation of the liquid portion of the enthalpy curve to the aging temperature T_a

$$\Delta H(T_a,t_\infty) = H(\mathrm{u},T_a) - H(\mathrm{liquid},T_a) = \int_{T_a}^{T}(\mathrm{Cp(liquid)} - \mathrm{Cp(u)})\,dT$$

with the upper limit of the integral $T > T_e$. The same approach was used by Petrie and Marshall,[31] who have analyzed the enthalpic aging data of a polystyrene sample in terms of a single effective relaxation time. Applying these authors' analysis to our experimental values of $\Delta H(T_a,t_a)$ for polystyrene, we recover exactly their reported value of the apparent activation energy for enthalpy relaxation in PS.

The values of β and τ are obtained by rearranging eq 3 to

$$\ln(-\ln f) = \beta \ln t_a - \beta \ln \tau$$

with $f \equiv \phi(t_a)$ symbolizing the fraction of enthalpy that remains unrelaxed at time t_a. If eq 1 displays a constant value of τ, a plot of ln (−ln f) versus ln t_a will yield a straight line with slope β and intercept $-\beta \ln \tau$.

Results and Discussion

Thermal characteristics of the samples in the glass transition region are shown in Table I. The total width $T_e - T_b$ is ca. 20–30 K, except for PTFC and HX2000, which display a broad transition over 75–80 K. Aging temperatures T_a, which are listed in Table II, are typically in the range $T_g - T_a$ = 10–20 K and may be located within the glass transition between T_g and T_b. This is illustrated in parts a–c of Figure 2, which show some representative heat capacity curves for unaged samples, plotted as a normalized, dimensionless heat capacity Cp(N) or fraction of heat capacity in excess of Cp(solid)

$$\mathrm{Cp(N)} = \frac{\mathrm{Cp(u)} - \mathrm{Cp(solid)}}{\mathrm{Cp(liquid)} - \mathrm{Cp(solid)}}$$

The familiar heat capacity overshoot at the upper edge of the glass transition is apparent in all cases, as a maximum in Cp(N) before the sample reaches the equilibrium liquid. In addition, a sub-T_g relaxation peak of the type commonly found in thermally quenched, high-enthalpy samples[32] may be observed, as illustrated in Figure 2c.

In the case of DDA9 and AZA9, the heat capacity increment at T_g listed in Table I depends on molecular mass and polydispersity as reported previously, reflecting the molecular mass dependence of Cp(liquid).[3] This dependence is stronger for DDA9 than AZA9, in tune with the general odd–even oscillation of physical properties imposed by spacer parity. For a given value of M, ΔCp tends to be higher for polydisperse samples than for fractions (compare AZA9*M*4200, a fraction, with AZA9-*M*8200, a polydisperse sample).

Parts a and b of Figure 3 show some typical heat capacity scans of aged samples, as a function of aging time t_a and

Table II
Numerical Data for Relaxation Kinetics of LCPs

sample	T_a (K)	$T_g - T_a$	ΔH_∞ (cal/g)	β^a	ln τ (min)
DDA9*M*2550	258	20	2.34	0.421	9.95
	263	15	1.68	0.388	8.62
	268	10	1.06	0.415	7.56
DDA9*M*6900	262	20	1.62	0.430	10.62
	267	15	1.18	0.463	9.50
	272	10	0.77	0.47*	8.5
DDA9*M*11300	265	20	1.30	0.217	14.69
	270	15	0.92	0.269	11.00
	275	10	0.56	0.265	8.90
AZA9*M*4200	260	27	2.51	0.166	19.89
	267	20	1.78	0.252	11.82
	272	15	1.27	0.295	8.89
	277	10	0.78	0.29*	6.7
AZA9*M*8200	271	20	1.52	0.342	10.68
	276	15	1.09	0.331	8.93
	281	10	0.68	0.333	5.60
AZA9*M*16900	273	20	1.48	0.225	12.80
	278	15	1.05	0.288	9.53
	282	11	0.76	0.41*	6.4
PTFC	324	20	1.34	0.298	11.78
	329	15	1.04	0.471	7.68
	334	10	0.73	0.494	5.90
HX2000	443	20	1.23	0.267	11.80
	461	2	0.41	0.398	5.32
PS	358	20	1.23	0.249	9.56
	363	15	0.92	0.300	6.60
	368	10	0.61	0.468	3.79

[a] Values of β are in the range $\beta \approx 0.02$–0.05, except as noted by an asterisk.

aging temperature T_a. The sub-T_g endothermal peaks that are a characteristic of enthalpy relaxation evolve in the manner previously described for conventional polymers, with respect to their magnitude and location. Figure 4 illustrates the aging time dependence of T_{max}, the sub-T_g peak maximum (a), and the width of the glass transition region (b). In general, the shape of the Cp(a) curves evolves with thermal history as already outlined in detail for polymers such as poly(vinyl chloride).[32]

Time dependence of f, the fraction of unrelaxed enthalpy, is illustrated in Figure 5, where representative values of f are plotted versus ln t_a at $T_g - T_a = 20$ K. While the LCP samples are roughly clustered together, polystyrene is relaxing much faster, on an absolute scale, although its molecular mass is comparatively very high (enthalpy relaxation rate of PS fractions was found to increase slightly with molecular mass up to a value of approximately 50 000[31]). As mentioned in the Experimental Section, our data on polystyrene are in exact agreement with values previously reported by Petrie and Marshall. Hedmark et al.,[6] in a recent study of physical aging in glassy LC poly(*p*-hydroxybenzoic acid-*co*-ethylene terephthalate) (HBA/ETP in a molar ratio of 0.6/0.4), similarly report a relaxation rate that is several orders of magnitude slower than in conventional polymers. However, direct comparison with the present data may not be possible, as morphology of the HBA/ETP polymer is biphasic, with isotropic and nematic domains.[33]

Representative values of $\Delta H(T_a,t_\infty)$ are given in Table II. Values of $\Delta H_\infty(T)$ exhibit a linear dependence on T_a, except in the immediate vicinity of T_g. For DDA9 and AZA9, dependence on molecular mass and polydispersity follows the same trend as ΔCp. Some typical plots of ln (−ln f) versus ln t_a are illustrated in Figure 6, and the values of β and ln τ extracted from these plots are summarized in Table II. Agreement with eq 3 is excellent, for the most part. However, the quality of the fit tends to decrease as the sample approaches equilibrium, e.g., close to T_g and/or at long aging times. Only the linear portion of the curve was used in such instances (see Figure 6b).

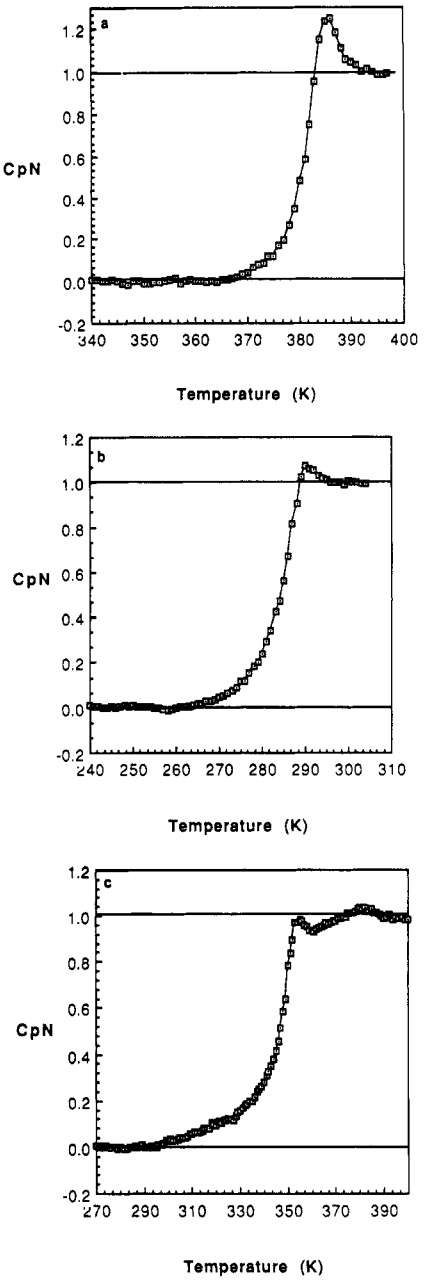

Figure 2. Representative heat capacity curves for unaged samples (plotted as Cp(N): (a) PS, (b) DDA9M11300, (c) PTFC.

Within the range $T_g - T_a$ up to ca. 20 K, ln τ varies with reciprocal aging temperature in a linear fashion, with a slope $x\Delta h^*/R$, where $x\Delta h^*$ (eq 2) may be considered as an activation energy in the glassy state at constant $T_f = T_g$. Values of $x\Delta h^*$ are listed in Table III.

Modeling of data over the entire relaxation curve will be addressed elsewhere, as the objective of the present study is limited to a comparison between the relaxation behavior of different LCP samples. Within the limitations of our computational approach, several observations may be made concerning results in Tables II and III.

At a given value of $T_g - T_a$, characteristic times τ are higher for all LCP samples than for PS. A drastic influence of molecular mass on kinetic parameters is apparent. A strong inverse correlation between ΔCp and ln τ is observed for the three DDA9 fractions, as expected (Figure 7). Polydisperse samples tend to relax somewhat faster than fractions of comparable molecular mass (compare fraction AZA9*M*4200 and polydisperse AZA9*M*800, for example),

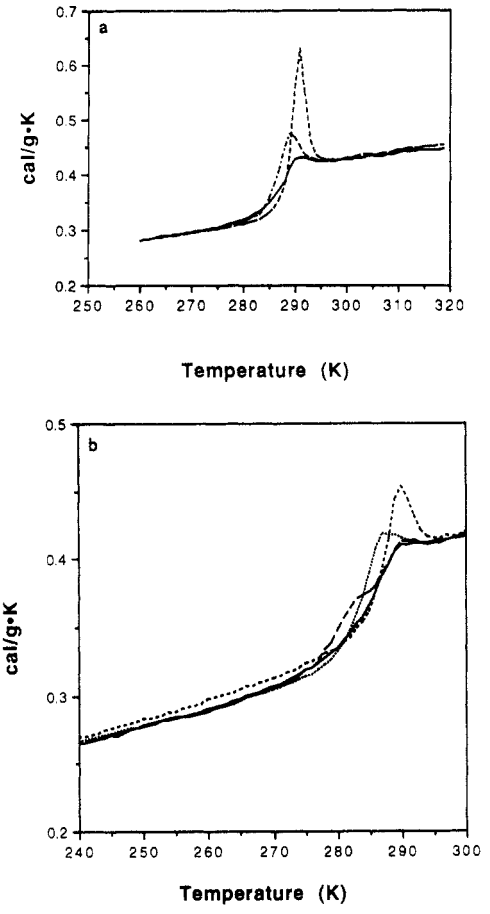

Figure 3. Evolution of heat capacity curves upon aging. (a) AZA9M169000 at T_a = 278 K ($T_g - T_a$ = 15 K). t_a: (—) 0 min, (– · –) 60 min, (– –) 430 min. (b) DDA9M11300 at t_a = 30 min. T_a: (—) unaged, (– –) 265 K, (· · ·) 270 K, (– · –) 275 K.

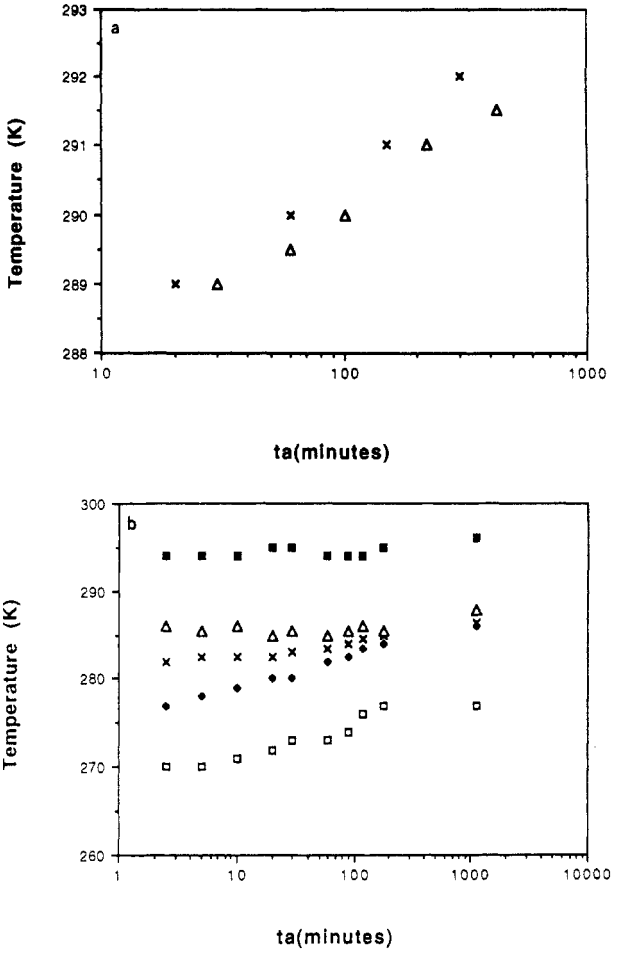

Figure 4. Aging time dependence of T_{max} and width of the glass transition region. (a) T_{max}, temperature of the sub-T_g relaxation peak maximum as a function of logarithmic aging time for AZA9M4200: (△) 270 K, (×) 272 K. (b) Width of the glass transition region and evolution of T_g with aging time for DDA9M6900 (T_a = 272 K): (□) T_b, (◆) T_1, (×) T_g, (△) T_2, (■) T_e.

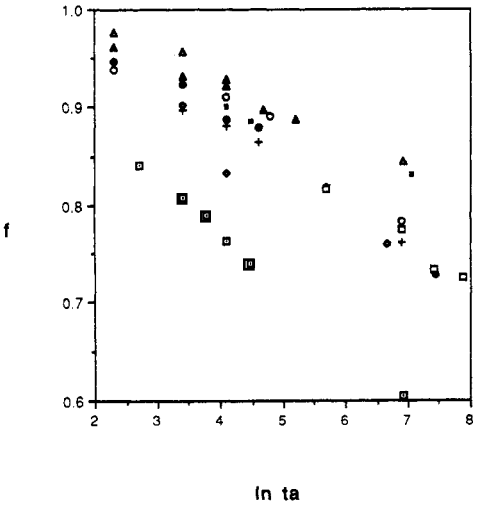

Figure 5. Fraction of unrelaxed enthalpy as a function of aging time for representative samples ($T_g - T_a$ = 20 K): (⊡) PS, (○) PTFC, (+) HX2000, (●) AZA9M8200, (□) AZA9M16900, (△) DDA9M2550, (▲) DDA9M6900, (■) DDA9M11300.

as was previously reported for polystyrene.[31] Semiflexible HX2000 and PTFC behave roughly as DDA9 and AZA9 of comparable chain length, with respect to ln τ. In making these comparisons, one should keep in mind the polydisperse nature and the broad glass transition of HX2000 and PTFC, which were both aged entirely above T_b (in the range Cp(N) ≈ 1.1–1.2). One should further note that PTFC and HX2000 glasses were obtained by quenching from the nematic phase, while AZA9 and DDA9 were quenched from the isotropic phase. Cheng et al.[5] have reported a somewhat larger value of β and τ upon quenching a nematic poly(azomethine) based on ethyleneoxy spacers from the nematic phase, compared to the isotropic phase. We know from previous investigations that the morphology of the nematic phase is strongly dependent on sample thermal history: the nematic phase is not in morphological equilibrium under normal experimental conditions[8] and, contrary to conventional polymers, LCPs usually keep a memory of their previous thermal history even after annealing well above T_g. This point will be addressed in more detail elsewhere. Preliminary experiments would seem to indicate that molecular mass effects are dominant, rather than inherent chain flexibility.

The values of β, which govern the time width of the relaxation spectrum, increase linearly with T_a in the case of PS, PTFC, and AZA9*M*16900, with a slope of ≈0.02/K (the distribution of relaxation times narrows as T_g is approached). A small increase with T_a is observed for AZA9*M*4200 and HX2000. The values of β for the remaining samples are independent of T_a, within experimental error, and appear to be dominated by molecular mass and molecular mass distribution.

Apparent activation energies $x\Delta h^*$ in the glassy state listed in Table III are also dependent on molecular weight and distribution in AZA9 and DDA9. The average activation energy Δh^* and, hence, the corresponding value of x have been separately estimated for PS, AZA9*M*4200, and PTFC (see Table III). Despite their low molecular mass, AZA9*M*4200 and PTFC display high values of Δh^*,

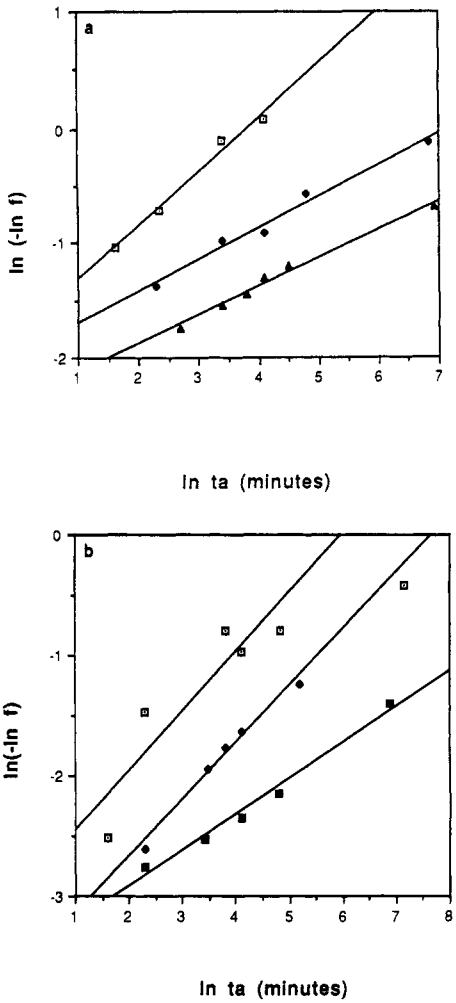

Figure 6. Representative plots of ln (-ln f) as a function of logarithmic aging time. Values of T_a are as shown. (a) PS: (⊡) 368, (◆) 363, (▲) 358. (b) PTFC [note that only short aging times are considered at T_a = 334 K (see text)]: (⊡) 334 K, (◆) 239 K, (■) 324 K.

Table III
Activation Energy in the Glassy State

	$x\Delta h^*$ (kJ/mol)	x	Δh^*
DDA9*M*2550	137		
DDA9*M*6900	121		
DDA9*M*11300	352		
AZA9*M*4200	316	0.24	1310[a]
AZA9*M*8000	319		
AZA9*M*16900	465		
PTFC	533	0.35	1520[a]
PS	600	0.68	880[b]
PVC[c]	187	0.10	1870

[a] Obtained from the dependence of T_g on cooling rate.[24] d ln $|q|$/d$(1/T_g)$ = $-\Delta h^*/R$. [b] Obtained from the relationship between Δh^* and the molecular weight of PS fractions in ref 34. [c] Values for poly(vinyl chloride) are from ref 35.

even approaching in the latter case the exceptionally highvalue reported for poly(vinyl chloride). A high level of cooperativity must be involved in the structural recovery process of LCPs, even in the case of inherently flexible chains such as AZA9. The rough inverse correlation between Δh^* and x, that seems to be a ubiquitous characteristic of glasses,[35] is also evident.

In summary, by extracting the equilibrium relaxation enthalpy ΔH_∞ in an independent manner (from the heat capacity curve of an unaged sample), we can rather accurately extract the characteristic time and the parameter β from a relatively small portion of the relaxation curve. The relaxation rate of LCPs is considerably slower than that of polystyrene. Kinetic parameters are strongly dependent on molecular mass and molecular mass distribution and do not appear to be dominated by inherent chain flexibility. This may be easily understood if one remembers the "rigidification" of inherently flexible chains in the nematic phase, as discussed in the introduction. However, definitive conclusions concerning the role of inherent chain flexibility may not be drawn from our current data.

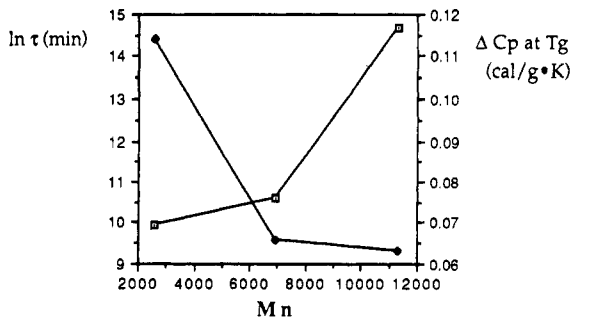

Figure 7. Values of ln τ and ΔCp for DDA9 ($T_g - T_a$ = 20 K): (-⊡-) ln τ, (-◆-) ΔCp.

The Narayanaswami equation follows an Arrhenius form within our range of aging temperatures. The apparent activation energy Δh^* seems to be rather high and the relaxation process strongly structure dependent. The parameter β which characterizes the distribution of relaxation times, with a small value implying a broad distribution, is nearly independent of (or weakly dependent on) T_a in some instances and linearly dependent on T_a in others. A more comprehensive discussion and modeling of relaxation behavior must await additional experiments. In particular, one should keep in mind that the meaning and value of β, τ, and x obtained by means of the simple parametrization described here may be different from the meaning and value of the corresponding parameter computed from the generalized form of eq 1.

Acknowledgment. This work was supported by NSF Grant DMR-8823084 and NSF Grant DMR-8908762. We are grateful to Dr. Russell Gaudiana for donating the PTFC polymer and to Dr. Richard Ikeda for donating the HX2000 polymer.

References and Notes

(1) Grebowicz, J.; Wunderlich, B. *J. Polym. Sci., Polym. Phys. Ed.* **1983**, *21*, 141.
(2) Cheng, S. Z. D.; Janimak, J. J.; Sridhar, K.; Harris, F. W. *Polym. Prepr. (Am. Chem. Soc., Div. Polym. Chem.)* **1990**, *31* (1), 251.
(3) Blumstein, R. B.; Kim, D. Y.; McGowan, C. B. *Liquid Crystalline Polymers*; ACS Symposium Series 294; Weiss, R. A., Ober, C. K., Eds.; American Chemical Society: Washington, DC, 1990.
(4) McGowan, C. B.; Kim, D. Y.; Blumstein, R. B. *Polym. Prepr. (Am. Chem. Soc., Div. Polym. Chem.)* **1990**, *31* (1), 251.
(5) Cheng, S. Z. D.; Janimak, J. J.; Lipinski, T. M.; Sridhar, K.; Huang, X. Y.; Harris, F. W. *Polymer* **1990**, *31*, 1122.
(6) Hedmark, P. G.; Dick, R. W. R.; Gedde, U. *Polym. Bull.* **1990**, *23*, 83.
(7) Müller, K.; Meier, P.; Kothe, G. *Prog. NMR Spectrosc.* **1985**, *17*, 211.
(8) Blumstein, R. B.; Blumstein, A. *Mol. Cryst. Liq. Cryst.* **1988**, *165*, 361.
(9) Müller, K.; Schleicher, A.; Ohmes, E.; Ferrarini, A.; Kothe, G. *Macromolecules* **1987**, *20*, 2761.
(10) Blumstein, A.; Lin, M. C.; Mithal, A. K.; Tayebi, A. *J. Appl. Polym. Sci.* **1990**, *41*, 995.
(11) Shaw, R. *Chem. Eng. Data* **1969**, *14*, 461.
(12) Loufakis, K.; Wunderlich, B. *J. Phys. Chem.* **1988**, *92*, 4205.
(13) For the definition of a "strong liquid", see: Angell, C. A. Reference 25.
(14) Esnault, P.; Galland, D.; Volino, F.; Blumstein, R. B. *Macromolecules* **1989**, *22*, 3137.

(15) d'Allest, J. F.; Maissa, P.; ten Bosch, A.; Sixou, P.; Blumstein, A.; Blumstein, R. B. *Phys. Rev. Lett.* **1988**, *61* (22), 2562.
(16) Sinta, R.; Gaudiana, R. A.; Minns, R. A.; Rogers, H. G. *Macromolecules* **1987**, *20* (10), 2374–2382.
(17) Ratto, J. A.; Volino, F.; Blumstein, R. B. *Macromolecules* **1991**, *24*, 2862.
(18) Ikeda, R., private communication.
(19) Moynihan, C. T.; Easteal, A. J.; Debolt, M. A. *J. Am. Ceram. Soc.* **1976**, *59*, 12.
(20) Kovacs, A. J.; Aklonis, J. J.; Hutchinson, J. M.; Ramos, A. R. *J. Polym. Phys.* **1979**, *17*, 1097.
(21) Tool, A. G. *J. Am. Ceram. Soc.* **1946**, *29*, 240.
(22) Narayanaswami, O. S. *J. Am. Ceram. Soc.* **1971**, *54*, 497.
(23) Hodge, I. M.; Berens, A. R. *Macromolecules* **1982**, *15*, 762.
(24) Scherer, G. W. *Relaxation in Glass and Composites*; John Wiley: New York, 1986.
(25) *Relaxation in Complex Systems*; Ngai, K. L., Wright, G. B., Eds.; U.S. Government Printing Office: Washington, DC, 1985.
(26) Moynihan, C. T.; Crichton, S. N.; Opalka, S. M. *J. Non-Cryst. Solids* **1991**, *131–133*, 420.
(27) Tribone, J. J.; O'Reilly, J. M.; Greener, J. *Macromolecules* **1986**, *19*, 1732–1739.
(28) Klein, T.; Hong, X. J.; Esnault, P.; Blumstein, A.; Volino, F. *Macromolecules* **1989**, *22*, 3731.
(29) Cheng, S. Z. D.; Cao, M. Y.; Wunderlich, B. *Macromolecules* **1986**, *19*, 1898.
(30) Cowie, J. M.; Ferguson, R. *Macromolecules* **1989**, *22*, 2307–2312.
(31) Marshall, A. S.; Petrie, S. E. B. *J. Appl. Phys.* **1975**, *46* (10), 4223.
(32) Berens, A.; Hodge, I. M. *Macromolecules* **1982**, *15*, 756.
(33) Gedde, U. W.; Buerger, D.; Boyd, R. H. *Macromolecules* **1987**, *20*, 988.
(34) Privalko, V. P.; Demchenko, S. S.; Lipatov, Y. S. *Macromolecules* **1986**, *19*, 901.
(35) Hodge, I. M. *Structure Relaxation and Physical Aging in Glassy Polymers*. Roe, R. J., O'Reilly, J. M., Eds.; *Mater. Res. Soc. Symp. Proc.* **1991**, *215*, 11.

Registry No. AZA9 (copolymer), 82764-72-5; AZA9 (SRU), 82851-48-7; DDA9 (copolymer), 78993-01-8; DDA9 (SRU), 79079-27-9; PTFC (copolymer), 109977-42-6; PTFC (SRU), 102819-40-9; HX2000, 141255-69-8.